

OSR1-sensitive regulation of Na^+/H^+ exchanger activity in dendritic cells

Venkanna Pasham,* Anand Rotte,* Wenting Yang, Christine Zelenak, Madhuri Bhandaru, Michael Föller, and Florian Lang

Department of Physiology, University of Tübingen, Tübingen, Germany

Submitted 29 November 2011; accepted in final form 23 May 2012

Pasham V, Rotte A, Yang W, Zelenak C, Bhandaru M, Föller M, Lang F. OSR1-sensitive regulation of Na^+/H^+ exchanger activity in dendritic cells. *Am J Physiol Cell Physiol* 303: C416–C426, 2012. First published May 30, 2012; doi:10.1152/ajpcell.00420.2011.—The oxidative stress-responsive kinase 1 (OSR1) is activated by WNK (with no K kinases) and in turn stimulates the thiazide-sensitive Na-Cl cotransporter (NCC) and the furosemide-sensitive Na-K-2Cl cotransporter (NKCC), thus contributing to transport and cell volume regulation. Little is known about extrarenal functions of OSR1. The present study analyzed the impact of decreased OSR1 activity on the function of dendritic cells (DCs), antigen-presenting cells linking innate and adaptive immunity. DCs were cultured from bone marrow of heterozygous WNK-resistant OSR1 knockin mice (*osr^{KI}*) and wild-type mice (*osr^{WT}*). Cell volume was estimated from forward scatter in FACS analysis, ROS production from 2',7'-dichlorodihydrofluorescein-diacetate fluorescence, cytosolic pH (pH_i) from 2',7'-bis-(2-carboxyethyl)-5-(and-6)-carboxyfluorescein fluorescence, and Na^+/H^+ exchanger activity from Na^+ -dependent realkalinization following ammonium pulse and migration utilizing transwell chambers. DCs expressed WNK1, WNK3, NCC, NKCC1, and OSR1. Phosphorylated NKCC1 was reduced in *osr^{KI}* DCs. Cell volume and pH_i were similar in *osr^{KI}* and *osr^{WT}* DCs, but Na^+/H^+ exchanger activity and ROS production were higher in *osr^{KI}* than in *osr^{WT}* DCs. Before LPS treatment, migration was similar in *osr^{KI}* and *osr^{WT}* DCs. LPS (1 $\mu\text{g}/\text{ml}$), however, increased migration of *osr^{WT}* DCs but not of *osr^{KI}* DCs. Na^+/H^+ exchanger 1 inhibitor cariporide (10 μM) decreased cell volume, intracellular reactive oxygen species (ROS) formation, Na^+/H^+ exchanger activity, and pH_i to a greater extent in *osr^{KI}* than in *osr^{WT}* DCs. LPS increased cell volume, Na^+/H^+ exchanger activity, and ROS formation in *osr^{WT}* DCs but not in *osr^{KI}* DCs and blunted the difference between *osr^{KI}* and *osr^{WT}* DCs. Na^+/H^+ exchanger activity in *osr^{WT}* DCs was increased by the NKCC1 inhibitor furosemide (100 nM) to values similar to those in *osr^{KI}* DCs. Oxidative stress (10 μM tert-butylhydroperoxide) increased Na^+/H^+ exchanger activity in *osr^{WT}* DCs but not in *osr^{KI}* DCs and reversed the difference between genotypes. Cariporide virtually abrogated Na^+/H^+ exchanger activity in both genotypes and blunted LPS-induced cell swelling and ROS formation in *osr^{WT}* mice. In conclusion, partial OSR1 deficiency influences Na^+/H^+ exchanger activity, ROS formation, and migration of dendritic cells.

intracellular pH_i ; cariporide; oxidative stress-responsive kinase 1; oxidative stress; cell volume

THE OXIDATIVE STRESS-RESPONSIVE KINASE 1 (OSR1) participates in the signaling of transport regulation during oxidative and osmotic stress (17, 37, 59, 66, 69, 83). The kinase is activated by the WNK (with no K) kinases WNK1 and WNK4, which are in turn activated by hyperosmotic stress (59, 79, 91). OSR1 stimulates the thiazide-sensitive Na-Cl cotransporter (NCC) and the furosemide-sensitive Na-K-2Cl cotransporter (NKCC) and thus influences cell volume, transepithelial transport, renal salt excretion, and GABA

neurotransmission (2, 15, 16, 27, 35–37, 59, 80). Mutations of WNK1 and WNK4 may lead to hypertension (20, 24, 37, 74, 84) and autonomic neuropathy (37). OSR1 is similarly considered to participate in the regulation of blood pressure (28, 77–79). Accordingly, OSR1 has been suggested as a potential drug target in the treatment of hypertension (28, 59, 77). The putative role of OSR1 in the regulation of immune cell function, remains, however, elusive.

The present study explored the role of OSR1 in the regulation of cell volume and formation of reactive oxygen species (ROS) in dendritic cells (DCs), antigen-presenting cells involved in the initiation of both innate and adaptive immunity and thus decisive for the regulation of the immune response (1, 3, 23, 58, 76). Exposure of DCs to bacterial wall components such as lipopolysaccharide (LPS) triggers generation of ROS (6, 49, 88), which contributes to pathogen defense (56). Similar to what has been shown in other cell types (25) including macrophages (13), ROS production is paralleled by H^+ generation, which in turn inhibits ROS-generating NADPH oxidase (33). Regulation of cytosolic pH (pH_i) involves the Na^+/H^+ exchanger in a wide variety of cells (13, 53, 55, 90) including macrophages (14, 32, 44, 71, 72) and monocytes (22, 38, 71). The Na^+/H^+ exchanger further participates in the regulation of cell volume (34, 42, 53).

The present study explored the impact of WNK-dependent OSR1 regulation on Na^+/H^+ exchanger activity, cell volume, and ROS formation in bone marrow-derived DCs.

MATERIALS AND METHODS

Animals. All animal experiments were conducted according to the German law for the welfare of animals and were approved by local authorities. Dendritic cells were cultured from bone marrow (87) of 7- to 11-wk-old heterozygous OSR1 knockin mice (*osr^{KI}*) and respective wild-type mice (*osr^{WT}*). The mice were kindly provided by D. Alessi (Univ. of Dundee, Dundee, UK). As described earlier (57), the knockin mice carry a mutation of the T-loop Thr residue in OSR1 (Thr185) to Ala preventing activation by WNK isoforms. Mice had free access to control diet (Ssniff, Soest, Germany) and tap drinking water.

Cell culture. Bone marrow-derived cells were flushed out of the cavities of the femur and tibia with PBS. Cells were then washed twice with RPMI 1640 medium and seeded out at a density of 2×10^6 cells per 60-mm dish (85). Cells were cultured for 6 days in RPMI 1640 (GIBCO, Darmstadt, Germany) containing 10% fetal calf serum (FCS), 1% penicillin-streptomycin, 1% glutamine, 1% non-essential amino acids, and 0.05% β -mercaptoethanol. Cultures were supplemented with granulocyte-macrophage colony-stimulating factor (GM-CSF; 35 ng/ml, Preprotech, Hamburg, Germany) and fed with fresh medium containing GM-CSF on days 3 and 6. On day 7, >85% of the cells expressed CD11c, which is a marker for mouse DCs (85–87). Experiments were performed on days 7–8 of DC culture.

Immunostaining and flow cytometry. Cells (4×10^5) were incubated in 100 μl FACS buffer [phosphate-buffered saline (PBS) plus 0.1% FCS] containing fluorochrome-conjugated antibodies at a con-

* V. Pasham and A. Rotte contributed equally and thus share first authorship.

Address for reprint requests and other correspondence: F. Lang, Dept. of Physiology, Univ. of Tübingen, Gmelinstr. 5, D-72076 Tübingen, Germany (e-mail: florian.lang@uni-tuebingen.de).

centration of 10 $\mu\text{g/ml}$ (86). A total of 2×10^4 cells were analyzed. Staining with FITC-conjugated anti-mouse CD11c (BD Pharmingen, Heidelberg, Germany) was used as a positive marker for dendritic cells. After incubating with the antibody for 60 min at 4°C, the cells were washed twice and resuspended in FACS buffer for flow cytometric analysis.

Real-time PCR. To evaluate OSR1 transcript levels, mRNA abundance was determined by quantitative real-time PCR. To this end, total RNA was isolated using the Trifast Reagent (Peqlab, Erlangen, Germany). RNA (2 μg) was reverse-transcribed using oligo(dT)₁₂₋₁₈ primers and SuperScript II Reverse Transcriptase (Invitrogen, Karlsruhe, Germany). Then, quantitative real-time PCR with the Bio-Rad iCycler iQ Real-Time PCR Detection System (Bio-Rad, Munich, Germany) was applied using the TaqMan Gene Expression Assay (Hs00362901 m1, Applied Biosystems) to determine OSR1 transcript levels. Reactions were performed using Universal TaqMan Master Mix (Applied Biosystems) in a final volume of 20 μl containing 2 μl of cDNA and the TaqMan Gene Expression Assay as recommended by the manufacturer. Following an initial incubation at 50°C for 2 min and 95°C for 10 min, 40 cycles of thermal cycling at 95°C for 15 s and 60°C for 60 s were performed. Calculated mRNA expression levels were normalized to the expression levels of TBP (Applied Biosystems) in the same cDNA sample. Relative quantification of gene expression was calculated according to the $\Delta\Delta\text{Ct}$ method.

Western blotting. DCs (2×10^6 cells) were washed twice with PBS, then solubilized in lysis buffer (Pierce) containing protease inhibitor cocktail (Sigma-Aldrich, Schnellendorf, Germany). Samples were stored at -80°C until use for Western blotting. Cell lysates were separated by 7.5% SDS-PAGE and blotted on nitrocellulose membranes. The blots were blocked with 5% BSA in triethanolamine-buffered saline (TBS) and 0.1% Tween 20. Then the blots were probed overnight with anti p-NKCC1 (21) (1:5,000) and GAPDH

(1:1,000, Cell Signaling) antibodies diluted in 5% milk in PBS and 0.1% Tween 20, washed 5 times, probed with secondary antibodies conjugated with horseradish peroxidase (1:2,000) for 1 h at room temperature, and washed final 5 times. Antibody binding was detected with the enhanced chemiluminescence (ECL) kit (Amersham, Freiburg, Germany). Densitometer scans of the blots were performed using Quantity One (Bio-Rad).

Treatments. Cells were exposed either to bacterial LPS (1 $\mu\text{g/ml}$) or to *t*-butyl hydroperoxide (TBOOH, 10 μM) in the presence or absence of cariporide (10 μM). Stock solutions of LPS were prepared in culture medium whereas the rest of the substances were dissolved in sterile distilled water. The cells were treated by adding the substances to the cell suspension at the indicated final concentration and incubated at 37°C in a humidified 5% CO₂ atmosphere.

Determination of cell volume. Cell volume was estimated from forward scatter in flow cytometric analysis. Briefly, 8×10^5 cells were taken in a culture dish and treated with LPS in the presence and absence of cariporide (10 μM). After the treatment, cells were collected and centrifuged, the pellet was resuspended in FACS buffer, and the forward scatter was analyzed on a FACSCalibur (Becton-Dickinson, Heidelberg, Germany).

Determination of ROS production. ROS production in DCs was determined utilizing 2',7'-dichlorodihydrofluorescein diacetate (DCFDA) (68). Briefly, 8×10^5 cells were taken in a culture dish and treated with LPS in the presence or absence of cariporide (10 μM). After the treatment, cells were collected and DCFDA (Sigma, Schnellendorf, Germany) was added to the cell suspension at a final concentration of 10 μM . After 30 min of incubation in the dark at 37°C, cells were centrifuged and the pellet was washed twice with ice-cold PBS. The pellet was then resuspended in FACS buffer and the fluorescence was analyzed with flow cytometry (FACSCalibur). DCFDA fluorescence intensity was measured in FL-1 with an excitation wavelength of 488 nm and an emission wavelength of 530 nm.

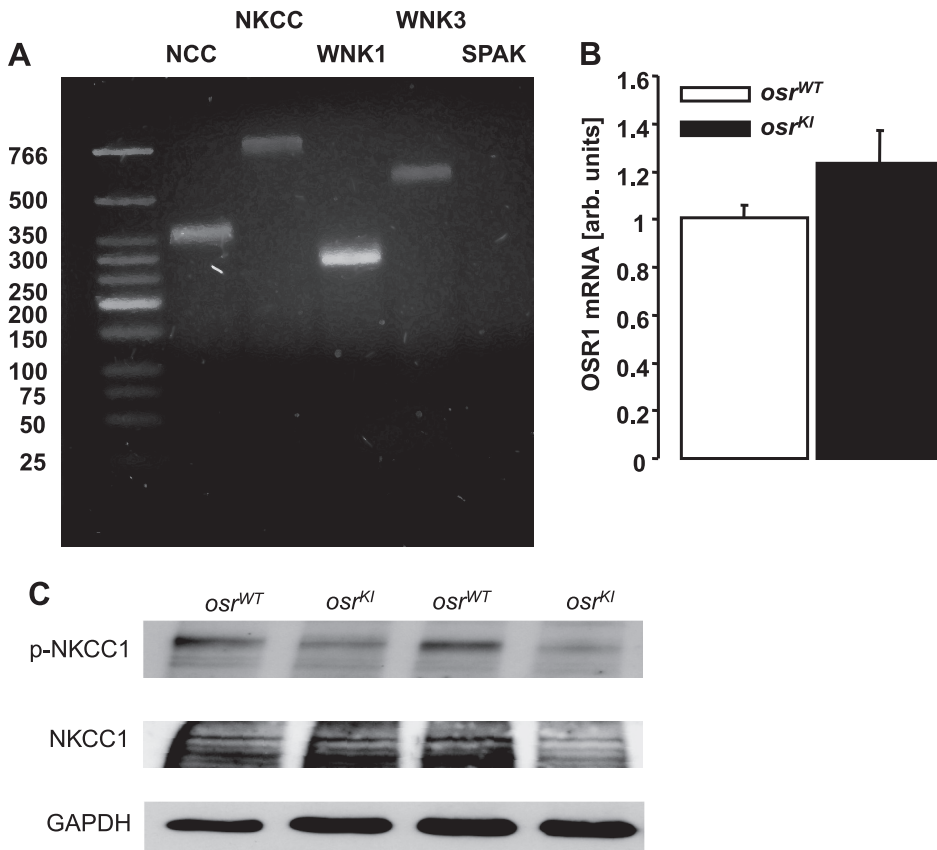


Fig. 1. WNK (with no K kinases) signaling pathway in murine bone marrow-derived dendritic cells (DCs). **A**: agarose gel visualizing the products of RT-PCR reactions amplifying Na-Cl cotransporter (NCC), Na-K-2Cl cotransporter (NKCC), WNK1, WNK3, and SPAK from cDNA of murine DCs. **B**: arithmetic means \pm SE ($n = 5$ mice) of relative oxidative stress-responsive kinase 1 (OSR1) mRNA abundance in murine DCs from heterozygous OSR1 knockin mice (*osr^{KI}*) and wild-type mice (*osr^{WT}*). **C**: original Western blot illustrating the expression of phosphorylated and total NKCC1 in DCs from heterozygous OSR1 knockin mice (*osr^{KI}*) and wild-type mice (*osr^{WT}*).

Measurement of intracellular pH. For digital imaging of pH_i , the cells were incubated in a HEPES-buffered Ringer solution containing $10 \mu\text{M}$ 2',7'-bis-(carboxyethyl)-5(6)-carboxyfluorescein-acetoxymethyl ester (BCECF-AM, Molecular Probes, Leiden, The Netherlands) for 15 min at 37°C . After loading, the chamber was flushed for 5 min with Ringer solution to remove any deesterified dye (63). The perfusion chamber was mounted on the stage of an inverted microscope (Zeiss Axiovert 135), which was used in the epifluorescence mode with a $\times 40$ oil immersion objective (Zeiss Neoplan). BCECF was successively excited at 490/10 and 440/10 nm, and the resultant fluorescent signal was monitored at 535/10 nm using an intensified charge-coupled device camera (Proxitronic) and specialized computer software (Metafluor). Between 10 and 20 cells were outlined and monitored during the course of the measurements. The results from each cell were averaged and taken for final analysis. Intensity ratio (490/440) data were converted into pH_i values using the high- K^+ /nigericin calibration technique (81). To this end, the cells were perfused at the end of each experiment for 5 min with standard high- K^+ /nigericin ($10 \mu\text{g/ml}$) solution (pH 7.0). The intensity ratio

data thus obtained were converted into pH values using the r_{max} , r_{min} , pK_a values previously generated from calibration experiments to obtain a standard nonlinear curve (pH range 5 to 8.5).

For acid loading, cells were transiently exposed to a solution containing 20 mM NH_4Cl leading to initial alkalinization of pH_i due to entry of NH_3 and binding of H^+ to form NH_4^+ (61). The acidification of pH_i upon removal of ammonia allowed calculation of the mean intrinsic buffering power (β) of the cells (61). Assuming that NH_4^+ and NH_3 are in equilibrium in cytosolic and extracellular fluid and that ammonia leaves the cells as NH_3 :

$$\beta = \Delta[\text{NH}_4^+]_i / \Delta p\text{H}_i$$

where $\Delta p\text{H}_i$ is the decrease of pH_i following ammonia removal and $\Delta[\text{NH}_4^+]_i$ is the decrease of cytosolic NH_4^+ concentration, which is identical to the concentration of $[\text{NH}_4^+]_i$ immediately before the removal of ammonia. The pK for $\text{NH}_4^+/\text{NH}_3$ is 8.9 (9) and at an extracellular pH of 7.4 the NH_4^+ concentration in extracellular fluid ($[\text{NH}_4^+]_o$) is 19.37 mM [$20/(1 + 10^{p\text{H}_o - pK})$]. The intracellular NH_4^+ concentration ($[\text{NH}_4^+]_i$) was calculated from:

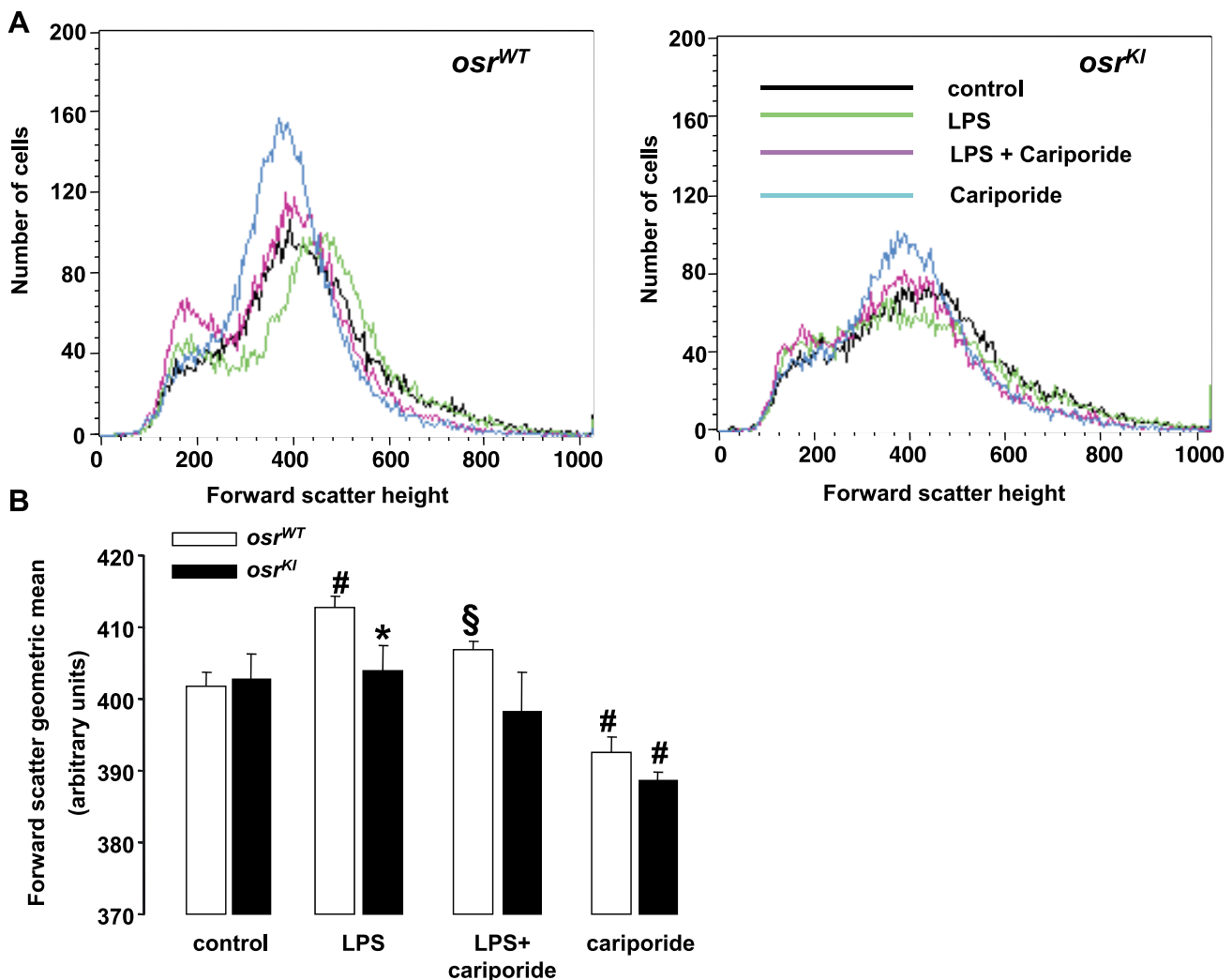


Fig. 2. Forward scatter of DCs from *osr^{KI}* and *osr^{WT}* mice following administration of LPS in the presence and absence of cariporide. **A:** representative FACS histograms depicting forward scatter in DCs from heterozygous OSR1 knockin mice (*osr^{KI}*, right) and from wild-type mice (*osr^{WT}*, left) without treatment (control, black line) and after a 4-h treatment with LPS ($1 \mu\text{g/ml}$) in the absence (green line) and presence (pink line) of cariporide or in the presence of cariporide alone (blue line). **B:** arithmetic means \pm SE ($n = 6$ independent experiments) of forward scatter in DCs from heterozygous OSR1 knockin mice (*osr^{KI}*, black bars) and from wild-type mice (*osr^{WT}*, white bars) before or 4 h following exposure to LPS ($1 \mu\text{g/ml}$) in the absence or presence of cariporide ($10 \mu\text{M}$) or in the presence of cariporide alone. *Significant difference ($P < 0.05$) from *osr^{WT}* DCs; #significant difference ($P < 0.01$) from respective control value; § $P < 0.05$, significant difference from respective absence of cariporide.

$$[\text{NH}_4]_i = 19.37 \cdot 10^{\text{pH}_o - \text{pH}_i} \text{ mM}$$

To calculate the $\Delta\text{pH}/\text{min}$ during realkalinization, a manual linear fit was placed over a narrow pH range (pH 6.7 to 6.9) which could be applied to all measured cells.

The solutions were composed of the following (in mM): standard HEPES: 115 NaCl, 5 KCl, 1 CaCl₂, 1.2 MgSO₄, 2 NaH₂PO₄, 10 glucose, and 32.2 HEPES; sodium-free HEPES: 132.8 NMDG, 3 KCl, 1 CaCl₂, 1.2 MgSO₄, 2 KH₂PO₄, 32.2 HEPES, 10 mannitol, and 10 glucose (for sodium-free ammonium chloride, 10 mM NMDG and mannitol were replaced with 20 mM NH₄Cl); and high K⁺ for calibration: 105 KCl, 1 CaCl₂, 1.2 MgSO₄, 32.2 HEPES, 10 mannitol, and 5 μM nigericin. The pH of the solutions was titrated to 7.4 or 7.0 with HCl/NaOH, HCl/NMDG and HCl/KOH, respectively, at 37°C.

Determination of migration. For migration assays, transwell inserts (BD Falcon 353097) and BD BioCoat Matrigel Invasion Chambers (354480, BD Biosciences) were used with a pore diameter size of 8 μm . The transwells were placed in a 24-well cell culture plate containing cell culture medium (750 μl) with or without chemokine ligand 21 (CCL21,

250 ng/ml, Peprotech) in the lower chamber. The upper chambers were filled with 500 μl cell culture medium containing DCs at a concentration of 50,000 cells/ml. The chamber was placed in a 5% CO₂ 37°C incubator for 4 h. In the following, the nonmigrated cells were removed by scrubbing with a cotton-tipped swab for two times and washing with PBS. The membrane was removed with a scalpel and fixed in 4% paraformaldehyde for 15 min. The migrated cells were then identified by staining with 4',6-diamidino-2-phenylindole (DAPI).

Statistics. Data are provided as means \pm SE, and *n* represents the number of independent experiments. All data were tested for significance using Student's unpaired two-tailed *t*-test, and only results with *P* < 0.05 were considered statistically significant.

RESULTS

To determine the presence of a functional WNK signaling pathway in murine bone marrow-derived DCs, RT-PCR was performed. As shown in Fig. 1A, DCs express WNK1, WNK3, NCC, and NKCC1 but not SPAK. As illustrated in Fig. 1B, OSR1

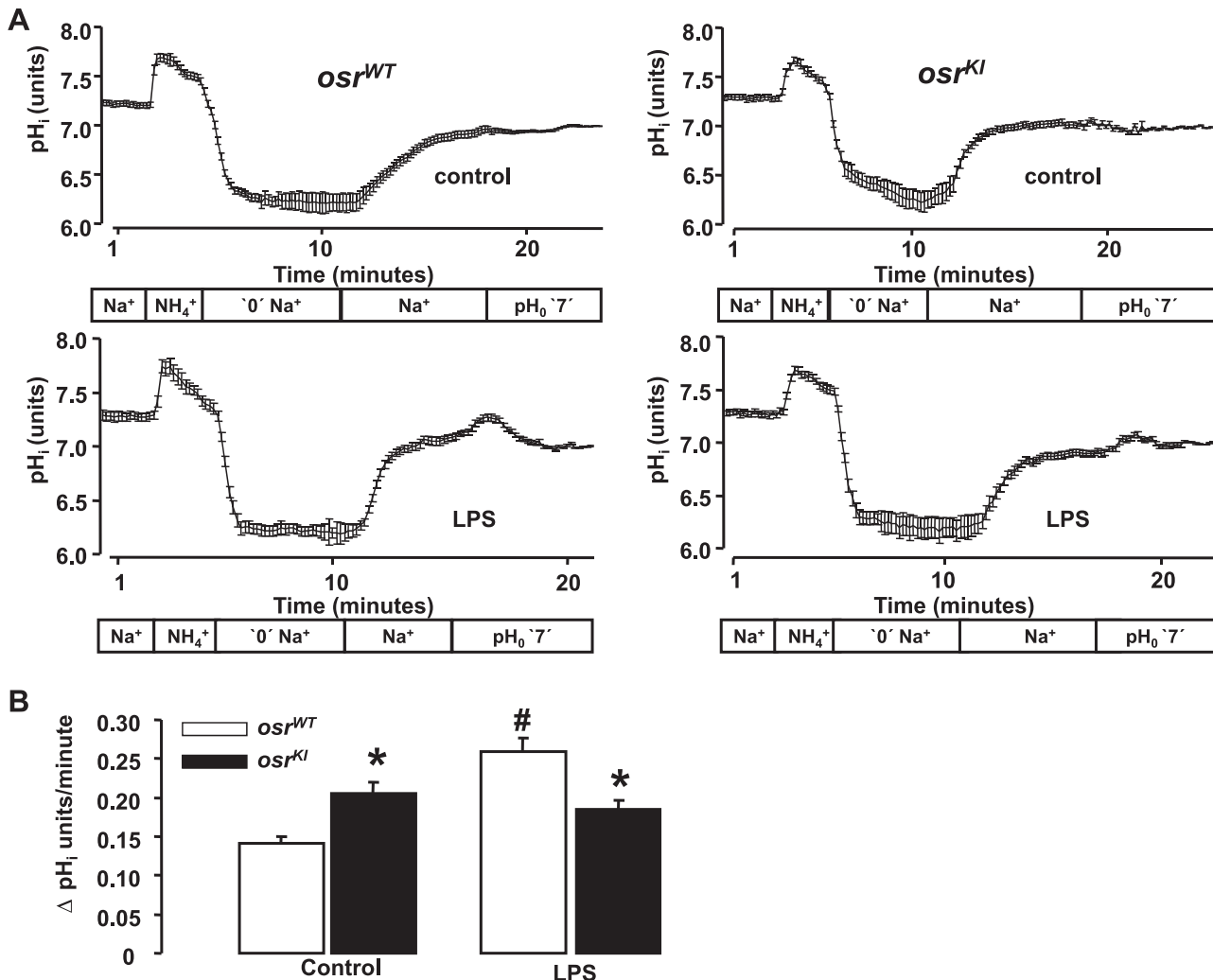


Fig. 3. Cytosolic pH (pH_i) recovery in DCs from *osr*^{KI} and *osr*^{WT} mice before and following LPS treatment. **A:** alterations of cytosolic pH in bone marrow-derived DCs following an ammonium pulse. To load the cells with H⁺, 20 mM NH₄Cl was added and Na⁺ was removed (replaced by NMDG) in a first step (see bars below each tracing), NH₄Cl was removed in a second step, Na⁺ was added in a third step, and nigericin [extracellular pH (pH_o) 7.0] was applied in a fourth step to calibrate each individual experiment. Representative experiments show the time-dependent alterations of cytosolic pH in DCs from heterozygous OSR1 knockin mice (*osr*^{KI}, right) and from wild-type mice (*osr*^{WT}, left) before (top) or following (bottom) a 4-h treatment with LPS (1 $\mu\text{g}/\text{ml}$). **B:** arithmetic means \pm SE (*n* = 6 independent experiments) of Na⁺-dependent recovery of cytosolic pH ($\Delta\text{pH}/\text{min}$) following an ammonium pulse in DCs from heterozygous OSR1 knockin mice (*osr*^{KI}, black bars) and from wild-type mice (*osr*^{WT}, white bars) before (left bars) or following (right bars) a 4-h treatment with LPS (1 $\mu\text{g}/\text{ml}$). *Significant difference (*P* < 0.01) from *osr*^{WT} DCs; #significant difference (*P* < 0.01) from respective value before LPS exposure.

mRNA is readily detectable in DCs and the transcript levels were similar in DCs from OSR1 knockin mice (*osr^{KI}*) and DCs from wild-type mice (*osr^{WT}*). Furthermore, the phosphorylation of NKCC1 was lower in *osr^{KI}* DCs (Fig. 1C), indicative of reduced OSR1 activity in *osr^{KI}* DCs.

As OSR1 is involved in regulatory cell volume increase, the present study determined the forward scatter of DCs in FACS analysis as a measure of cell volume. As illustrated in Fig. 2, no significant difference was observed in forward scatter between *osr^{KI}* and *osr^{WT}*. Treatment of the DCs with LPS was followed within 4 h by an increase in forward scatter of *osr^{WT}* DCs, pointing to an increase in cell volume (Fig. 2). In contrast, the forward scatter of *osr^{KI}* DCs was not significantly modified by LPS treatment. As a result, following LPS treatment, forward scatter was significantly higher in *osr^{WT}* DCs than in *osr^{KI}* DCs. To elucidate the contribution of the Na⁺/H⁺ exchanger, experiments were performed in the absence or presence of cariporide, a specific inhibitor of Na⁺/H⁺ exchanger 1 (NHE1) (48). As a result, in both genotypes, forward scatter was significantly decreased following treatment of DCs with cariporide (Fig. 2). The decrease of forward scatter tended to be higher in *osr^{KI}* DCs than in *osr^{WT}* DCs, a difference, however, not reaching statistical significance.

The lack of cell shrinkage in untreated *osr^{KI}* DCs could have been due to lack of OSR1, NCC, and/or NKCC expression in *osr^{WT}* DCs or due to a compensatory increase in Na⁺/H⁺ exchanger activity of *osr^{KI}* DCs. To explore that possibility, cytosolic pH was determined in DCs utilizing BCECF fluorescence. The Na⁺/H⁺ exchanger activity was determined with the ammonium pulse technique (61). To this end, NH₄Cl was added to the perfusate, leading to NH₃ entry into the cells, binding of H⁺ to form NH₄⁺ and thus to transient cytosolic alkalization (Fig. 3). The subsequent removal of NH₄Cl was followed by exit of NH₃ leaving H⁺ behind. The H⁺ thus

retained within the cell led to cytosolic acidification (Fig. 3). In the absence of Na⁺, the average cytosolic pH declined further after an ammonium pulse, indicating that the cells did not express significant Na⁺-independent H⁺ extrusion mechanisms to maintain or recover cytosolic pH (Table 1). Addition of Na⁺ was, however, followed by rapid pH recovery, pointing to the operation of the Na⁺/H⁺ exchanger. The Na⁺-dependent pH recovery was blunted in the presence of NHE1 inhibitor cariporide (Table 1). According to the ammonium pulse, the Na⁺/H⁺ exchanger activity was significantly higher in *osr^{KI}* DCs than in *osr^{WT}* DCs.

Treatment of *osr^{WT}* DCs with LPS (1 μg/ml) was followed within 4 h by a significant increase in Na⁺-dependent realkalization (Table 1 and Fig. 3). Again, in the absence of Na⁺, further acidification was observed, i.e., accelerated realkalization following LPS treatment was due to Na⁺-dependent H⁺ extrusion, pointing to stimulation of Na⁺/H⁺ exchanger activity (Fig. 3). The increase in Na⁺/H⁺ exchanger activity was blunted in the presence of the NHE1 inhibitor cariporide (10 μM) (Table 1). In contrast to what was observed in *osr^{WT}* DCs, treatment of *osr^{KI}* DCs with LPS did not significantly modify Na⁺/H⁺ exchanger activity. Accordingly, following LPS treatment, Na⁺/H⁺ exchanger activity was significantly lower in *osr^{KI}* DCs than in *osr^{WT}* DCs (Fig. 3). Thus, LPS treatment reversed the difference between the genotypes (Fig. 3).

To determine whether inhibition of NKCC1 with furosemide in *osr^{WT}* DCs mimics the effects seen in *osr^{KI}* mice, *osr^{WT}* DCs were treated with furosemide (100 nM) and Na⁺/H⁺ exchanger activity was studied. As seen in Fig. 4, treatment of DCs with furosemide led to a significant increase in basal Na⁺/H⁺ exchanger activity. In analogy to what had been observed in *osr^{KI}* DCs, the LPS-induced stimulation of Na⁺/H⁺ exchanger activity was reversed in the presence of furosemide (Fig. 4).

Table 1. Cytosolic pH (ΔpH_i), buffer capacity, and sodium-independent pH recovery in bone marrow-derived dendritic cells isolated from OSR1 knockin mice and from wild-type mice before (control) and following a 4-h treatment with lipopolysaccharide (1 μg/ml) or a 2-h treatment with *t*-butyl hydroperoxide (10 μM) in the absence or presence of cariporide (10 μM)

	Intracellular pH, units	Buffer Capacity, mM/pH unit	Sodium-Independent pH Recovery, ΔpH units/min	Sodium-Dependent pH Recovery (NHE Activity), ΔpH units/min	No. of Cells
Control					
<i>osr^{WT}</i>	7.33 ± 0.01	15.8 ± 0.9	-0.066 ± 0.007	0.141 ± 0.009	199
<i>osr^{KI}</i>	7.35 ± 0.01	15.1 ± 1.1	-0.055 ± 0.009	0.206 ± 0.015*	150
Cariporide alone					
<i>osr^{WT}</i>	7.28 ± 0.03	18.3 ± 1.5	-0.070 ± 0.008	0.032 ± 0.012‡	41
<i>osr^{KI}</i>	7.26 ± 0.04	17.8 ± 1.4	-0.044 ± 0.022	0.012 ± 0.004‡	40
LPS 4 h					
<i>osr^{WT}</i>	7.35 ± 0.01	14.5 ± 2.2	-0.053 ± 0.006	0.259 ± 0.018†	200
<i>osr^{KI}</i>	7.33 ± 0.01	14.4 ± 0.9	-0.065 ± 0.006	0.185 ± 0.012*	172
LPS 4 h + cariporide					
<i>osr^{WT}</i>	7.31 ± 0.03	13.7 ± 3.4	-0.071 ± 0.030	0.026 ± 0.004‡	46
<i>osr^{KI}</i>	7.34 ± 0.01	13.6 ± 1.4	-0.042 ± 0.006	0.019 ± 0.004‡	40
TBOOH					
<i>osr^{WT}</i>	7.24 ± 0.02†	16.0 ± 1.4	-0.054 ± 0.014	0.229 ± 0.027†	77
<i>osr^{KI}</i>	7.23 ± 0.02†	14.0 ± 1.2	-0.061 ± 0.011	0.186 ± 0.019†	98
TBOOH + cariporide					
<i>osr^{WT}</i>	6.99 ± 0.04‡	14.3 ± 1.2	-0.044 ± 0.017	0.026 ± 0.009‡	42
<i>osr^{KI}</i>	6.99 ± 0.02‡	15.7 ± 1.4	-0.068 ± 0.017	0.022 ± 0.008‡	47

Values are means ± SE. *osr^{KI}*, oxidative stress-responsive kinase 1 (OSR1) knockin mice; *osr^{WT}*, wild-type mice; LPS, lipopolysaccharide; TBOOH, *t*-butyl hydroperoxide; NHE, Na⁺/H⁺ exchanger. *Significant difference ($P < 0.05$) from the respective wild-type value; †significant difference ($P < 0.05$) from the respective control value; ‡significant difference ($P < 0.05$) from the absence of cariporide.

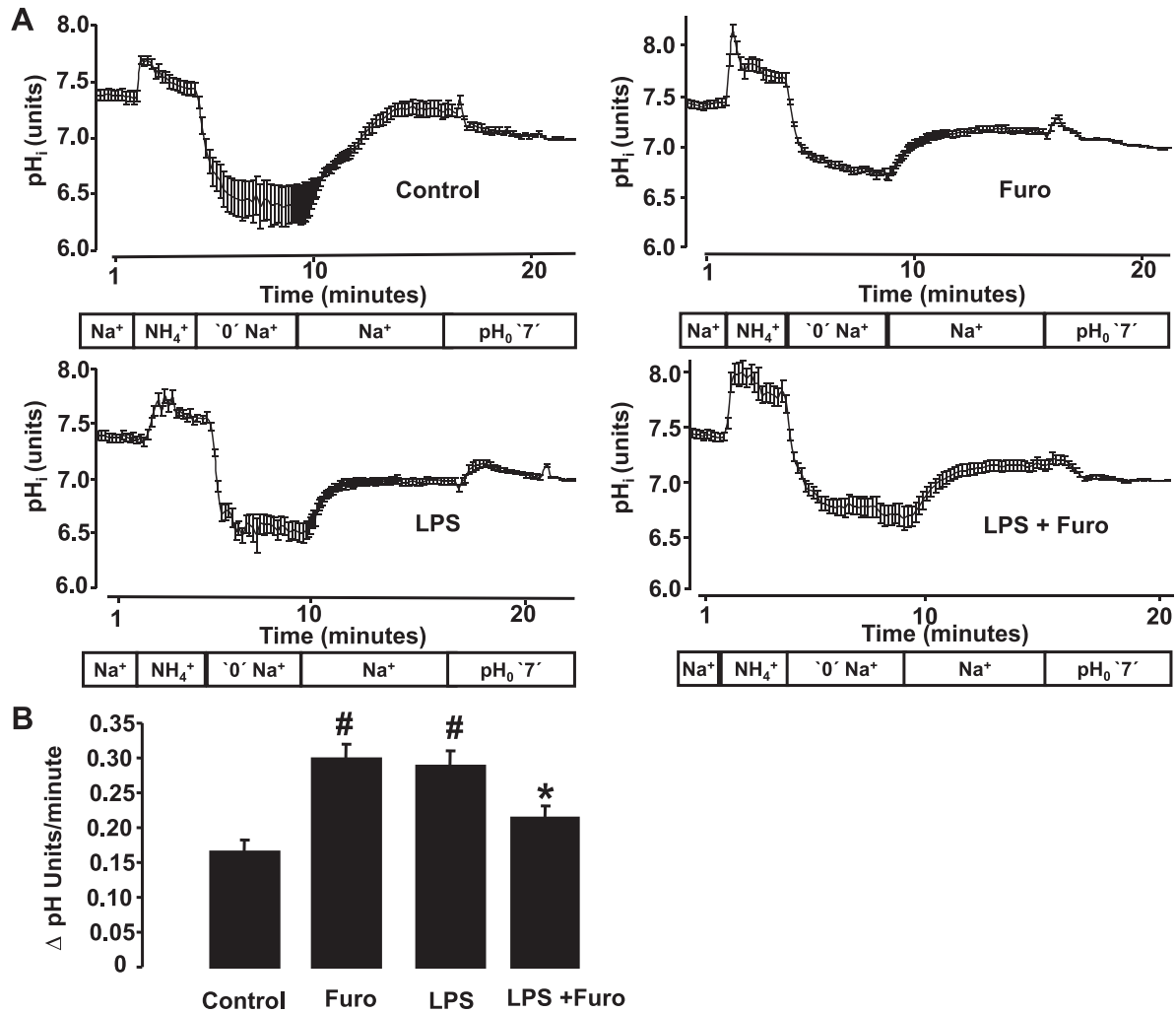


Fig. 4. Cytosolic pH recovery in DCs from *osr*^{WT} mice before and following LPS treatment in the presence and absence of furosemide (Furo). *A*: representative experiments showing the time-dependent alterations of cytosolic pH in DCs from heterozygous OSR1 wild-type mice before (*top*) or following (*bottom*) a 4-h treatment with LPS (1 μ g/ml) in the presence (*right*) and absence of furosemide (100 nM). *B*: arithmetic means \pm SE ($n = 6$ independent experiments) of Na⁺-dependent recovery of cytosolic pH in DCs (Δ pH/min) following an ammonium pulse in DCs from wild-type mice before (control) or following 4-h treatment with LPS (1 μ g/ml) in the presence and absence of furosemide (100 nM). #Significant difference ($P < 0.01$) from control DCs; *significant difference ($P < 0.01$) from respective absence of LPS.

LPS-induced ROS formation has previously been shown to account for the LPS-induced stimulation of Na⁺/H⁺ exchanger activity (62). Therefore, the effect of oxidative stress on Na⁺/H⁺ exchanger activity was studied. Treatment of *osr*^{WT} DCs for 2 h with TBOOH (10 μ M) to induce oxidative stress was followed by a significant increase in Na⁺-dependent realkalinization (Table 1 and Fig. 5). Again, in the absence of Na⁺, no acidification was observed, i.e., accelerated realkalinization following LPS treatment was due to Na⁺-dependent H⁺ extrusion pointing to stimulation of Na⁺/H⁺ exchanger activity (Fig. 5). As is apparent from Table 1, the increase in Na⁺/H⁺ exchanger activity was blunted in the presence of the NHE1 inhibitor cariporide (10 μ M). In contrast to *osr*^{WT} DCs, treatment of *osr*^{KI} DCs with TBOOH did not significantly modify Na⁺/H⁺ exchanger activity. Following TBOOH treatment, Na⁺/H⁺ exchanger activity was significantly lower in *osr*^{KI} DCs than in *osr*^{WT} DCs (Fig. 5). Thus, similar to LPS, TBOOH reversed the difference between the genotypes (Fig. 5).

The buffer capacity of the cells was not significantly different between *osr*^{KI} DCs and *osr*^{WT} DCs and was not significantly modified by exposure to LPS or oxidative stress (Table 1).

Additional studies addressed the role of OSR1 and/or NHE1 in LPS-induced ROS formation. As illustrated in Fig. 6, before LPS treatment, ROS formation was significantly higher in *osr*^{KI} DCs than in *osr*^{WT} DCs. Cariporide treatment did not affect the intracellular ROS in *osr*^{WT} DCs but significantly decreased ROS formation in *osr*^{KI} DCs (Fig. 6). LPS enhanced the ROS formation in *osr*^{WT} DCs but did not significantly alter ROS formation in *osr*^{KI} DCs. Accordingly, following LPS treatment, ROS formation was not significantly different between *osr*^{KI} DCs and *osr*^{WT} DCs (Fig. 6).

The migratory potential of DCs is dependent on NHE1 activity. Thus, further experiments addressed the CCL21-induced migration of control- and LPS-(1 μ g/ml) treated DCs. As presented in Fig. 7, migration of DCs from *osr*^{KI} mice tended to be less pronounced than migration of DCs from wild-type mice under con-

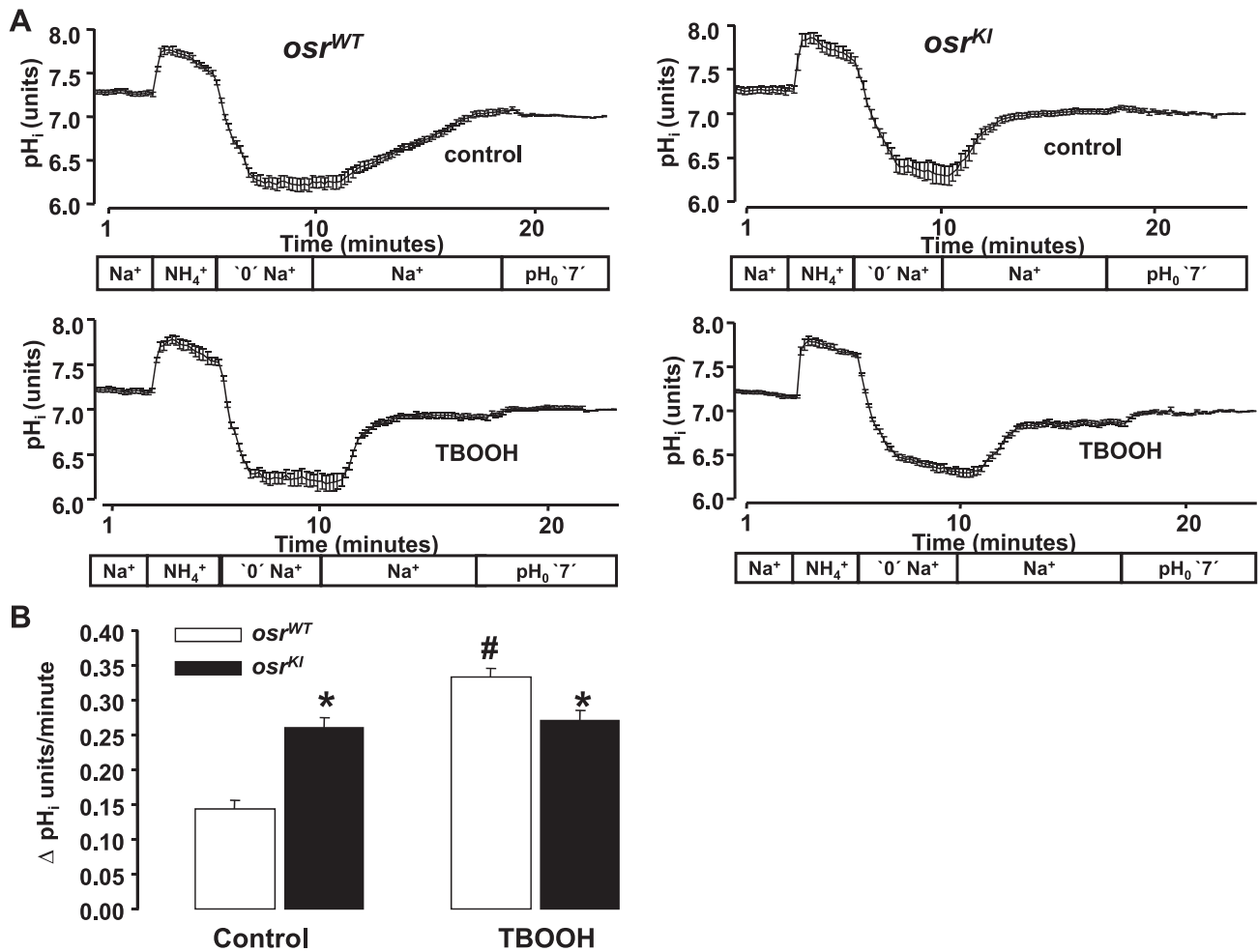


Fig. 5. Cytosolic pH recovery in DCs from *osr^{KI}* and *osr^{WT}* mice before and following exposure to *t*-butyl hydroperoxide (TBOOH). *A*: representative experiments showing the time-dependent alterations of cytosolic pH in DCs from heterozygous OSR1 knockin mice (*osr^{KI}*, right) and from wild-type mice (*osr^{WT}*, left) before (top) or following (bottom) a 2-h treatment with TBOOH (10 μ M). *B*: arithmetic means \pm SE ($n = 6$ independent experiments) of Na⁺-dependent recovery of cytosolic pH (Δ pH/min) following an ammonium pulse in DCs from heterozygous OSR1 knockin mice (*osr^{KI}*, black bars) and from wild-type mice (*osr^{WT}*, white bars) before (control, left bars) or following a 2-h treatment with TBOOH (10 μ M, right bars). *Significant difference ($P < 0.01$) from *osr^{WT}* DCs; #significant difference ($P < 0.01$) from control.

control conditions, a difference, however, not reaching statistical significance. LPS treatment markedly stimulated migration of *osr^{WT}* DCs but did not significantly affect migration of *osr^{KI}* DCs. Accordingly, upon LPS treatment, migration of *osr^{KI}* DCs was significantly less pronounced than migration of *osr^{WT}* DCs (Fig. 7).

DISCUSSION

The present study reveals that WNK resistance of OSR1 affects Na⁺/H⁺ exchanger activity and formation of ROS in DCs. In the absence of LPS, cell volume was similar in DCs from *osr^{KI}* and *osr^{WT}*, but Na⁺/H⁺ exchanger activity and formation of ROS were significantly higher in *osr^{KI}* DCs than in *osr^{WT}* DCs. Similar to what has been reported earlier (62), LPS triggered the formation of ROS, activated the Na⁺/H⁺ exchanger NHE1, and increased cell volume in *osr^{WT}* DCs. All of those effects were blunted or even absent in *osr^{KI}* DCs. Accordingly, LPS reversed the differences of ROS formation, Na⁺/H⁺ exchanger activity, and cell volume between *osr^{KI}* DCs and *osr^{WT}* DCs. The increase in Na⁺/H⁺ exchanger activity in *osr^{WT}* DCs following LPS treatment was virtually

abolished in the presence of cariporide, which inhibits both NHE1 and NHE2 (67). In DCs the NHE1, but not the NHE2, isoform is expressed (62).

As shown earlier (62), Na⁺/H⁺ exchanger activation by LPS depends on ROS activation. The signaling involves MAP kinases and phosphoinositide 3 kinase (82), well-known stimulators of Na⁺/H⁺ exchangers (8, 39, 43, 53, 73). Conversely, ROS production is sensitive to cytosolic pH (33). The higher cytosolic pH and Na⁺/H⁺ exchanger activity in *osr^{KI}* DCs thus presumably contributes to the higher ROS production in those cells. ROS production is in turn important for antimicrobial activity (56).

Na⁺/H⁺ exchanger activity is enhanced in *osr^{KI}* DCs despite the more alkaline pH, which should actually decrease Na⁺/H⁺ exchanger activity (29). At least in theory, the stimulation of the Na⁺/H⁺ exchanger in *osr^{KI}* DCs could result from cell volume regulation. Cell shrinkage leads to stimulation of the Na⁺/H⁺ exchanger, which operates in parallel to the Cl⁻/HCO₃⁻ exchanger (34, 40). Collectively, the two carriers accomplish the entry of NaCl, followed by osmotically obliged water. The H⁺

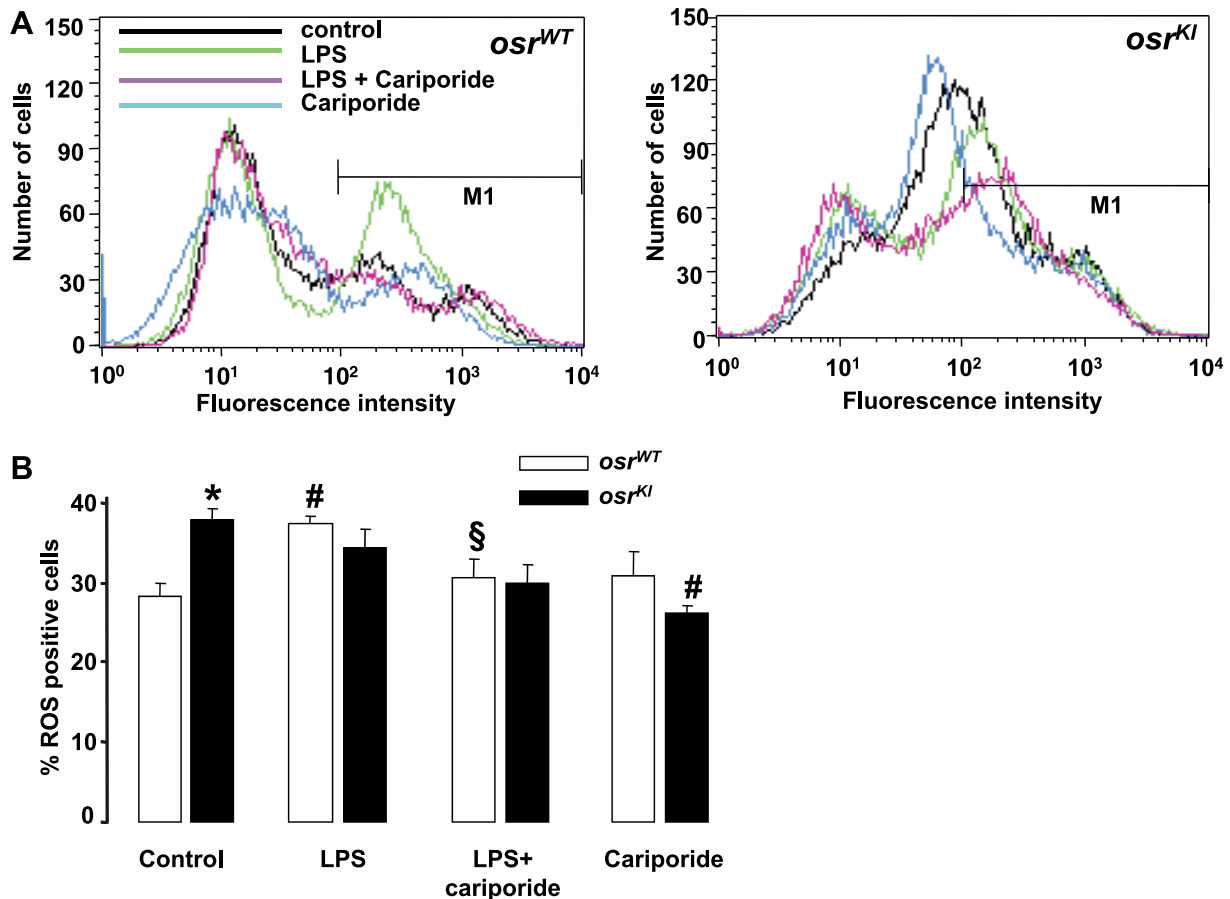


Fig. 6. Effect of LPS on reactive oxygen species (ROS) production of DCs from *osr^{KI}* and *osr^{WT}* mice in the presence and absence of cariporide. *A*: representative FACS histograms depicting ROS-dependent 2',7'-dichlorodihydrofluorescein diacetate (DCFDA) fluorescence in DCs from heterozygous OSR1 knockin mice (*osr^{KI}*, right) and from wild-type mice (*osr^{WT}*, left) without treatment (control, black line) and after a 4-h treatment with LPS (1 μ g/ml) in the absence (green line) and presence (pink line) of cariporide or in the presence of cariporide alone (blue line). *B*: arithmetic means \pm SE ($n = 6$ independent experiments) of the percentage of ROS-positive DCs from heterozygous OSR1 knockin mice (*osr^{KI}*, black bars) and from wild-type mice (*osr^{WT}*, white bars) before or 4 h following exposure to LPS (1 μ g/ml) in the absence or presence of cariporide (10 μ M) or in the presence of cariporide alone. *Significant difference ($P < 0.01$) from *osr^{WT}* DCs; #significant difference ($P < 0.01$) from respective control value; § $P < 0.05$, significant difference from respective absence of cariporide.

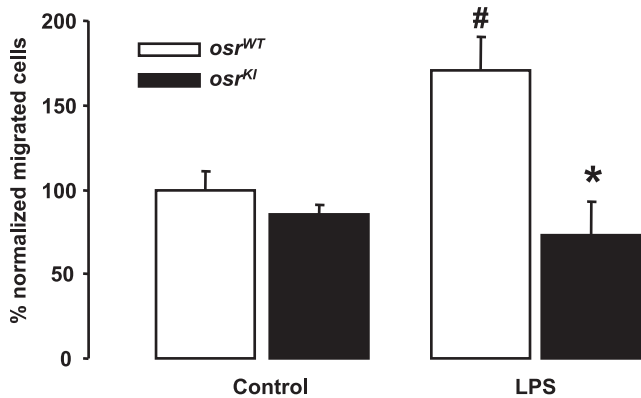


Fig. 7. Decreased migration of DCs from *osr^{KI}* mice. Arithmetic means \pm SE ($n = 6$ independent experiments) of the normalized migration of DCs from heterozygous OSR1 knockin mice (*osr^{KI}*, black bars) and from wild-type mice (*osr^{WT}*, white bars) following a 4-h treatment without (control, left bars) or with LPS (right bars). *Significant difference ($P < 0.05$) from *osr^{WT}* DCs; #significant difference ($P < 0.05$) from respective control values.

and HCO_3^- extruded in exchange for Na^+ (Na^+/H^+ exchanger) and Cl^- ($\text{Cl}^-/\text{HCO}_3^-$ exchanger) are osmotically not relevant as they are replenished in the cell by cytosolic formation from CO_2 , which easily crosses the cell membrane (34, 40). Along those lines, LPS-induced cell swelling was abolished in the presence of cariporide, an observation highlighting the impact of the Na^+/H^+ exchanger in cell volume regulation.

The cell volume regulatory stimulation of the Na^+/H^+ exchanger may be required because of the lacking OSR1-dependent stimulation of NKCC in *osr^{KI}* DCs. OSR1 is known to stimulate the NKCC and to participate in cell volume regulation (2, 15, 16, 27, 35–37, 59, 80). It is tempting to reason that OSR1 deficiency leads to decreased NKCC activity, requiring enhanced activity of the Na^+/H^+ exchanger for cell volume maintenance. We cannot rule out, however, the possibility that OSR1 regulates Na^+/H^+ exchanger directly, e.g., by phosphorylating the carrier protein. As furosemide treatment of *osr^{WT}* DCs similarly increases Na^+/H^+ exchanger activity, a decreased NKCC activity at least contributes to the upregulation of Na^+/H^+ exchanger activity.

Cell volume may influence the formation of ROS and antioxidative defense (30, 31, 64, 65), and cell shrinkage interferes with

ROS generation (62). Moreover, cytosolic pH modifies a variety of further functions, such as migration, cytokine release, adherence, nitric oxide formation, proliferation, and differentiation of macrophages and/or monocytes (5, 7, 10, 19, 44, 50–52, 54, 60, 71, 75). Na^+/H^+ exchanger activity further fosters (12, 26, 45, 46) or inhibits (4, 41, 47) apoptosis.

The present study did not address the functional significance of OSR1-sensitive DC function. DCs are antigen-presenting cells critically important in the regulation of innate and adaptive immunity (3, 18, 70, 89). To fulfill their diverse functions, DCs have to migrate into inflammatory tissues and return to secondary lymphoid sites following microbial challenge (11). The blunted stimulation of migration following LPS treatment is expected to compromise the function of *osr^{KI}* DCs. On the other hand, augmented ROS formation of *osr^{KI}* DCs is expected to foster the removal of pathogens (56). However, the difference of ROS formation between *osr^{KI}* and *osr^{WT}* DCs is lost following stimulation with LPS, and enhanced ROS production in immature DCs may not be relevant for the power of the immune response. Clearly, further studies will be required to elucidate the impact of reduced OSR1 activity on the immune system.

In conclusion, the present study disclosed that, in bone marrow-derived DCs, WNK resistance of OSR1 upregulates Na^+/H^+ exchanger activity, leading to cytosolic alkalization and fostering formation of ROS. The study thus reveals a completely novel functional consequence of OSR1 inhibition.

ACKNOWLEDGMENTS

Cariporide was a kind gift from Sanofi Aventis (Frankfurt, Germany), and the p-NKCC1 antibody (21) was a kind gift from Dr. Biff Forbush (Department of Cellular and Molecular Physiology, Yale University School of Medicine, New Haven, CT). The authors gratefully acknowledge the meticulous preparation of the manuscript by L. Subasic and S. Rube.

GRANTS

This work was supported by the Deutsche Forschungsgemeinschaft DFG (SFB 766).

DISCLOSURES

No conflicts of interest, financial or otherwise, are declared by the author(s).

AUTHOR CONTRIBUTIONS

V.P., A.R., W.Y., C.Z., and M.B. performed the experiments; V.P., A.R., W.Y., C.Z., M.B., M.F., and F.L. approved the final version of the manuscript; A.R. and F.L. conception and design of the research; A.R. and M.F. analyzed the data; A.R. and F.L. interpreted the results of the experiments; A.R. prepared the figures; M.F. and F.L. edited and revised the manuscript; F.L. drafted the manuscript.

REFERENCES

- Adler HS, Steinbrink K. Tolerogenic dendritic cells in health and disease: friend and foe! *Eur J Dermatol* 17: 476–491, 2007.
- Anselmo AN, Earnest S, Chen W, Juang YC, Kim SC, Zhao Y, Cobb MH. WNK1 and OSR1 regulate the Na^+ , K^+ , 2Cl^- cotransporter in HeLa cells. *Proc Natl Acad Sci USA* 103: 10883–10888, 2006.
- Banchereau J, Briere F, Caux C, Davoust J, Lebecque S, Liu YJ, Pulendran B, Palucka K. Immunobiology of dendritic cells. *Annu Rev Immunol* 18: 767–811, 2000.
- Barriere H, Poujeol C, Tauc M, Blasi JM, Counillon L, Poujeol P. CFTR modulates programmed cell death by decreasing intracellular pH in Chinese hamster lung fibroblasts. *Am J Physiol Cell Physiol* 281: C810–C824, 2001.
- Belloq A, Suberville S, Philippe C, Bertrand F, Perez J, Fouqueray B, Cherqui G, Baud L. Low environmental pH is responsible for the induction of nitric-oxide synthase in macrophages. Evidence for involvement of nuclear factor-kappaB activation. *J Biol Chem* 273: 5086–5092, 1998.
- Bergamo P, Maurano F, D'Arienzo R, David C, Rossi M. Association between activation of phase 2 enzymes and down-regulation of dendritic cell maturation by c9,t11-conjugated linoleic acid. *Immunol Lett* 117: 181–190, 2008.
- Bidani A, Reisner BS, Haque AK, Wen J, Helmer RE, Tuazon DM, Heming TA. Bactericidal activity of alveolar macrophages is suppressed by V-ATPase inhibition. *Lung* 178: 91–104, 2000.
- Boehmer C, Palmada M, Klaus F, Jeyaraj S, Lindner R, Laufer J, Daniel H, Lang F. The peptide transporter PEPT2 is targeted by the protein kinase SGK1 and the scaffold protein NHERF2. *Cell Physiol Biochem* 22: 705–714, 2008.
- Boyersky G, Ganz MB, Sterzel RB, Boron WF. pH regulation in single glomerular mesangial cells. I. Acid extrusion in absence and presence of HCO_3^- . *Am J Physiol Cell Physiol* 255: C844–C856, 1988.
- Cassatella MA, Flynn RM, Amezcua MA, Bazzoni F, Vicentini F, Trinchieri G. Interferon gamma induces in human neutrophils and macrophages expression of the mRNA for the high affinity receptor for monomeric IgG (Fc gamma R-1 or CD64). *Biochem Biophys Res Commun* 170: 582–588, 1990.
- Cavanagh LL, Von Andrian UH. Travellers in many guises: the origins and destinations of dendritic cells. *Immunol Cell Biol* 80: 448–462, 2002.
- Chakrabarti S, Hoque AN, Karmazyn M. A rapid ischemia-induced apoptosis in isolated rat hearts and its attenuation by the sodium-hydrogen exchange inhibitor HOE 642 (cariporide). *J Mol Cell Cardiol* 29: 3169–3174, 1997.
- De Vito P. The sodium/hydrogen exchanger: a possible mediator of immunity. *Cell Immunol* 240: 69–85, 2006.
- DeCoursey TE, Cherny VV. Voltage-activated proton currents in human THP-1 monocytes. *J Membr Biol* 152: 131–140, 1996.
- Delpire E, Austin TM. Kinase regulation of Na^+ - K^+ - 2Cl^- cotransport in primary afferent neurons. *J Physiol* 588: 3365–3373, 2010.
- Delpire E, Gagnon KB. SPAK and OSR1, key kinases involved in the regulation of chloride transport. *Acta Physiol (Oxf)* 187: 103–113, 2006.
- Delpire E, Gagnon KB. SPAK and OSR1: STE20 kinases involved in the regulation of ion homeostasis and volume control in mammalian cells. *Biochem J* 409: 321–331, 2008.
- Den Haan JM, Bevan MJ. A novel helper role for CD4 T cells. *Proc Natl Acad Sci USA* 97: 12950–12952, 2000.
- Dieter P, Schulze-Specking A, Karck U, Decker K. Prostaglandin release but not superoxide production by rat Kupffer cells stimulated in vitro depends on Na^+/H^+ exchange. *Eur J Biochem* 170: 201–206, 1987.
- Flatman PW. Cotransporters, WNKs and hypertension: an update. *Curr Opin Nephrol Hypertens* 17: 186–192, 2008.
- Flemmer AW, Monette MY, Djuricic M, Dowd B, Darman R, Gimenez I, Forbush B. Phosphorylation state of the Na^+ - K^+ - Cl^- cotransporter (NKCC1) in the gills of Atlantic killifish (*Fundulus heteroclitus*) during acclimation to water of varying salinity. *J Exp Biol* 213: 1558–1566, 2010.
- Forsbeck K, Nygren P, Larsson R, Nilsson M, Nilsson K, Gylfe E. Cytosolic pH is differently regulated in the monoblastic U-937 and erythroleukemic K-562 cell lines. *Exp Cell Res* 176: 96–106, 1988.
- Forster R, Davalos-Misslitz AC, Rot A. CCR7 and its ligands: balancing immunity and tolerance. *Nat Rev Immunol* 8: 362–371, 2008.
- Furgason SB, Linas S. Mechanisms of type I and type II pseudohypoaldosteronism. *J Am Soc Nephrol* 21: 1842–1845, 2010.
- Garciaarena CD, Caldiz CI, Correa MV, Schinella GR, Mosca SM, Chiappe de Cingolani GE, Cingolani HE, Ennis IL. Na^+/H^+ exchanger-1 inhibitors decrease myocardial superoxide production via direct mitochondrial action. *J Appl Physiol* 105: 1706–1713, 2008.
- Garciaarena CD, Caldiz CI, Portiansky EL, Chiappe de Cingolani GE, Ennis IL. Chronic NHE-1 blockade induces an antiapoptotic effect in the hypertrophied heart. *J Appl Physiol* 106: 1325–1331, 2009.
- Gimenez I. Molecular mechanisms and regulation of furosemide-sensitive Na^+ - K^+ - Cl^- cotransporters. *Curr Opin Nephrol Hypertens* 15: 517–523, 2006.
- Glover M, Oshaughnessy KM. SPAK and WNK kinases: a new target for blood pressure treatment? *Curr Opin Nephrol Hypertens* 20: 16–22, 2011.
- Grinstein S, Cohen S, Goetz JD, Rothstein A. Na^+/H^+ exchange in volume regulation and cytoplasmic pH homeostasis in lymphocytes. *Fed Proc* 44: 2508–2512, 1985.

30. Gulbins E, Welsch J, Lepple-Wienhuis A, Heinle H, Lang F. Inhibition of Fas-induced apoptotic cell death by osmotic cell shrinkage. *Biochem Biophys Res Commun* 236: 517–521, 1997.
31. Haussinger D, Lang F, Gerok W. Regulation of cell function by the cellular hydration state. *Am J Physiol Endocrinol Metab* 267: E343–E355, 1994.
32. Heming TA, Bidani A. Plasmalemmal H⁺ extruders in mammalian alveolar macrophages. *Comp Biochem Physiol A Mol Integr Physiol* 133: 143–150, 2002.
33. Henderson LM, Chappell JB, Jones OT. Internal pH changes associated with the activity of NADPH oxidase of human neutrophils. Further evidence for the presence of an H⁺ conducting channel. *Biochem J* 251: 563–567, 1988.
34. Hoffmann EK, Lambert IH, Pedersen SF. Physiology of cell volume regulation in vertebrates. *Physiol Rev* 89: 193–277, 2009.
35. Hoffmann EK, Schettino T, Marshall WS. The role of volume-sensitive ion transport systems in regulation of epithelial transport. *Comp Biochem Physiol A Mol Integr Physiol* 148: 29–43, 2007.
36. Huang CL, Yang SS, Lin SH. Mechanism of regulation of renal ion transport by WNK kinases. *Curr Opin Nephrol Hypertens* 17: 519–525, 2008.
37. Kahle KT, Rinehart J, Lifton RP. Phosphoregulation of the Na-K-2Cl and K-Cl cotransporters by the WNK kinases. *Biochim Biophys Acta* 1802: 1150–1158, 2010.
38. Ladoux A, Damais C, Krawiec I, Abita JP, Frelin C. An increase in intracellular pH is a general response of promonocytic cells to differentiating agents. *FEBS Lett* 234: 353–356, 1988.
39. Lang F, Bohmer C, Palmada M, Seebom G, Strutz-Seebom N, Vallon V. (Patho)physiological significance of the serum- and glucocorticoid-inducible kinase isoforms. *Physiol Rev* 86: 1151–1178, 2006.
40. Lang F, Busch GL, Ritter M, Volkl H, Waldegger S, Gulbins E, Haussinger D. Functional significance of cell volume regulatory mechanisms. *Physiol Rev* 78: 247–306, 1998.
41. Lang F, Madlung J, Bock J, Lukewille U, Kaltenbach S, Lang KS, Belka C, Wagner CA, Lang HJ, Gulbins E, Lepple-Wienhues A. Inhibition of Jurkat-T-lymphocyte Na⁺/H⁺-exchanger by CD95(Fas/Apo-1)-receptor stimulation. *Pflügers Arch* 440: 902–907, 2000.
42. Lang F, Ritter M, Woll E, Weiss H, Haussinger D, Hoflacher J, Maly K, Grunicke H. Altered cell volume regulation in ras oncogene expressing NIH fibroblasts. *Pflügers Arch* 420: 424–427, 1992.
43. Lang F, Strutz-Seebom N, Seebom G, Lang UE. Significance of SGK1 in the regulation of neuronal function. *J Physiol* 588: 3349–3354, 2010.
44. Lardner A. The effects of extracellular pH on immune function. *J Leukoc Biol* 69: 522–530, 2001.
45. Li S, Bao P, Li Z, Ouyang H, Wu C, Qian G. Inhibition of proliferation and apoptosis induced by a Na⁺/H⁺ exchanger-1 (NHE-1) antisense gene on drug-resistant human small cell lung cancer cells. *Oncol Rep* 21: 1243–1249, 2009.
46. Liu Z, Wang S, Zhou H, Yang Y, Zhang M. Na⁺/H⁺ exchanger mediates TNF-alpha-induced hepatocyte apoptosis via the calpain-dependent degradation of Bcl-xL. *J Gastroenterol Hepatol* 24: 879–885, 2009.
47. Maeno E, Takahashi N, Okada Y. Dysfunction of regulatory volume increase is a key component of apoptosis. *FEBS Lett* 580: 6513–6517, 2006.
48. Masereel B, Pochet L, Laeckmann D. An overview of inhibitors of Na⁺/H⁺ exchanger. *Eur J Med Chem* 38: 547–554, 2003.
49. Matsue H, Edelbaum D, Shalhevet D, Mizumoto N, Yang C, Mummert ME, Oeda J, Masayasu H, Takashima A. Generation and function of reactive oxygen species in dendritic cells during antigen presentation. *J Immunol* 171: 3010–3018, 2003.
50. Nemeth ZH, Mabley JG, Deitch EA, Szabo C, Hasko G. Inhibition of the Na⁺/H⁺ antiporter suppresses IL-12 p40 production by mouse macrophages. *Biochim Biophys Acta* 1539: 233–242, 2001.
51. Ohmori Y, Reynolds E, Hamilton TA. Modulation of Na⁺/K⁺ exchange potentiates lipopolysaccharide-induced gene expression in murine peritoneal macrophages. *J Cell Physiol* 148: 96–105, 1991.
52. Orlinska U, Newton RC. Modification of tumor necrosis factor-alpha (TNF-alpha) production by the Na⁺-dependent HCO₃⁻ cotransport in lipopolysaccharide-activated human monocytes. *Immunopharmacology* 30: 41–50, 1995.
53. Pedersen SF. The Na⁺/H⁺ exchanger NHE1 in stress-induced signal transduction: implications for cell proliferation and cell death. *Pflügers Arch* 452: 249–259, 2006.
54. Prpic V, Yu SF, Figueiredo F, Hollenbach PW, Gawdi G, Herman B, Uhing RJ, Adams DO. Role of Na⁺/H⁺ exchange by interferon-gamma in enhanced expression of JE and I-A beta genes. *Science* 244: 469–471, 1989.
55. Putney LK, Denker SP, Barber DL. The changing face of the Na⁺/H⁺ exchanger, NHE1: structure, regulation, and cellular actions. *Annu Rev Pharmacol Toxicol* 42: 527–552, 2002.
56. Rada BK, Geiszt M, Kaldi K, Timar C, Ligeti E. Dual role of phagocytic NADPH oxidase in bacterial killing. *Blood* 104: 2947–2953, 2004.
57. Rafiqi FH, Zuber AM, Glover M, Richardson C, Fleming S, Jovanovic S, Jovanovic A, O'Shaughnessy KM, Alessi DR. Role of the WNK-activated SPAK kinase in regulating blood pressure. *EMBO Mol Med* 2: 63–75, 2010.
58. Riccardi C, Bruscoli S, Migliorati G. Molecular mechanisms of immunomodulatory activity of glucocorticoids. *Pharmacol Res* 45: 361–368, 2002.
59. Richardson C, Alessi DR. The regulation of salt transport and blood pressure by the WNK-SPAK/OSR1 signalling pathway. *J Cell Sci* 121: 3293–3304, 2008.
60. Rolfe MW, Kunkel SL, Rowens B, Standiford TJ, Cragoe EJ Jr, Strieter RM. Suppression of human alveolar macrophage-derived cytokines by amiloride. *Am J Respir Cell Mol Biol* 6: 576–582, 1992.
61. Roos A, Boron WF. Intracellular pH. *Physiol Rev* 61: 296–434, 1981.
62. Rotte A, Pasham V, Eichenmuller M, Mahmud H, Xuan NT, Shumilina E, Gotz F, Lang F. Effect of bacterial lipopolysaccharide on Na⁺/H⁺ exchanger activity in dendritic cells. *Cell Physiol Biochem* 26: 553–562, 2010.
63. Rotte A, Pasham V, Eichenmuller M, Yang W, Qadri SM, Bhandaru M, Lang F. Regulation of basal gastric acid secretion by the glycogen synthase kinase GSK3. *J Gastroenterol* 45: 1022–1032, 2010.
64. Saha N, Schreiber R, vom DS, Lang F, Gerok W, Haussinger D. Endogenous hydroperoxide formation, cell volume and cellular K⁺ balance in perfused rat liver. *Biochem J* 296: 701–707, 1993.
65. Saha N, Stoll B, Lang F, Haussinger D. Effect of anisotonic cell-volume modulation on glutathione-S-conjugate release, t-butylhydroperoxide metabolism and the pentose-phosphate shunt in perfused rat liver. *Eur J Biochem* 209: 437–444, 1992.
66. Salter RD, Watkins SC. Dendritic cell altered states: what role for calcium? *Immunol Rev* 231: 278–288, 2009.
67. Scholz W, Albus U, Counillon L, Gogelein H, Lang HJ, Linz W, Weichert A, Scholkens BA. Protective effects of HOE642, a selective sodium-hydrogen exchange subtype 1 inhibitor, on cardiac ischaemia and reperfusion. *Cardiovasc Res* 29: 260–268, 1995.
68. Sinha A, Singh A, Satchidanandam V, Natarajan K. Impaired generation of reactive oxygen species during differentiation of dendritic cells (DCs) by *Mycobacterium tuberculosis* secretory antigen (MTSA) and subsequent activation of MTSA-DCs by mycobacteria results in increased intracellular survival. *J Immunol* 177: 468–478, 2006.
69. Solomon A, Bandhakavi S, Jabbar S, Shah R, Beitel GJ, Morimoto RI. *Caenorhabditis elegans* OSR-1 regulates behavioral and physiological responses to hyperosmotic environments. *Genetics* 167: 161–170, 2004.
70. Steinman RM, Nussenzweig MC. Avoiding horror autotoxicus: the importance of dendritic cells in peripheral T cell tolerance. *Proc Natl Acad Sci USA* 99: 351–358, 2002.
71. Swallow CJ, Grinstein S, Rotstein OD. Regulation and functional significance of cytoplasmic pH in phagocytic leukocytes. In: *Mechanisms of Leukocyte Activation, Current Topics in Membranes and Transport*, edited by Grinstein S and Rotstein OD. New York: Academic, 1990, p. 227–247.
72. Swallow CJ, Grinstein S, Sudsbury RA, Rotstein OD. Cytoplasmic pH regulation in monocytes and macrophages: mechanisms and functional implications. *Clin Invest Med* 14: 367–378, 1991.
73. Takahashi E, Abe J, Gallis B, Aebersold R, Spring DJ, Krebs EG, Berk BC. p90(RSK) is a serum-stimulated Na⁺/H⁺ exchanger isoform-1 kinase. Regulatory phosphorylation of serine 703 of Na⁺/H⁺ exchanger isoform-1. *J Biol Chem* 274: 20206–20214, 1999.
74. Uchida S. Pathophysiological roles of WNK kinases in the kidney. *Pflügers Arch* 460: 695–702, 2010.
75. Vairo G, Argyriou S, Bordun AM, Gonda TJ, Cragoe EJ Jr, Hamilton JA. Na⁺/H⁺ exchange involvement in colony-stimulating factor-1-stimulated macrophage proliferation. Evidence for a requirement during late G1 of the cell cycle but not for early growth factor responses. *J Biol Chem* 265: 16929–16939, 1990.

76. Van Duivenvoorde LM, Han WG, Bakker AM, Louis-Pence P, Charbonnier LM, Apparailly F, van der Voort EI, Jorgensen C, Huizinga TW, Toes RE. Immunomodulatory dendritic cells inhibit Th1 responses and arthritis via different mechanisms. *J Immunol* 179: 1506–1515, 2007.
77. Villa F, Deak M, Alessi DR, van Aalten DM. Structure of the OSR1 kinase, a hypertension drug target. *Proteins* 73: 1082–1087, 2008.
78. Villa F, Goebel J, Rafiqi FH, Deak M, Thastrup J, Alessi DR, van Aalten DM. Structural insights into the recognition of substrates and activators by the OSR1 kinase. *EMBO Rep* 8: 839–845, 2007.
79. Vitari AC, Deak M, Morrice NA, Alessi DR. The WNK1 and WNK4 protein kinases that are mutated in Gordon's hypertension syndrome phosphorylate and activate SPAK and OSR1 protein kinases. *Biochem J* 391: 17–24, 2005.
80. Vitari AC, Thastrup J, Rafiqi FH, Deak M, Morrice NA, Karlsson HK, Alessi DR. Functional interactions of the SPAK/OSR1 kinases with their upstream activator WNK1 and downstream substrate NKCC1. *Biochem J* 397: 223–231, 2006.
81. Waibren SJ, Geibel J, Boron WF, Modlin IM. Luminal perfusion of isolated gastric glands. *Am J Physiol Cell Physiol* 266: C1013–C1027, 1994.
82. Watts C, West MA, Zaru R. TLR signalling regulated antigen presentation in dendritic cells. *Curr Opin Immunol* 22: 124–130, 2010.
83. Wheeler JM, Thomas JH. Identification of a novel gene family involved in osmotic stress response in *Caenorhabditis elegans*. *Genetics* 174: 1327–1336, 2006.
84. Wilson FH, Disse-Nicodeme S, Choate KA, Ishikawa K, Nelson-Williams C, Desitter I, Gunel M, Milford DV, Lipkin GW, Achard JM, Feely MP, Dussol B, Berland Y, Unwin RJ, Mayan H, Simon DB, Farfel Z, Jeunemaitre X, Lifton RP. Human hypertension caused by mutations in WNK kinases. *Science* 293: 1107–1112, 2001.
85. Xuan NT, Shumilina E, Matzner N, Zemtsova IM, Biedermann T, Goetz F, Lang F. Ca^{2+} -dependent functions in peptidoglycan-stimulated mouse dendritic cells. *Cell Physiol Biochem* 24: 167–176, 2009.
86. Xuan NT, Shumilina E, Nasir O, Bobbala D, Gotz F, Lang F. Stimulation of mouse dendritic cells by Gum Arabic. *Cell Physiol Biochem* 25: 641–648, 2010.
87. Xuan NT, Shumilina E, Qadri SM, Gotz F, Lang F. Effect of thymoquinone on mouse dendritic cells. *Cell Physiol Biochem* 25: 307–314, 2010.
88. Yamada H, Arai T, Endo N, Yamashita K, Fukuda K, Sasada M, Uchiyama T. LPS-induced ROS generation and changes in glutathione level and their relation to the maturation of human monocyte-derived dendritic cells. *Life Sci* 78: 926–933, 2006.
89. Yamazaki S, Steinman RM. Dendritic cells as controllers of antigen-specific Foxp3+ regulatory T cells. *J Dermatol Sci* 54: 69–75, 2009.
90. Zachos NC, Tse M, Donowitz M. Molecular physiology of intestinal Na^+/H^+ exchange. *Annu Rev Physiol* 67: 411–443, 2005.
91. Zagorska A, Pozo-Guisado E, Boudeau J, Vitari AC, Rafiqi FH, Thastrup J, Deak M, Campbell DG, Morrice NA, Prescott AR, Alessi DR. Regulation of activity and localization of the WNK1 protein kinase by hyperosmotic stress. *J Cell Biol* 176: 89–100, 2007.

